

This is a repository copy of *Prediction of alkaline earth elements in bone remains by near infrared spectroscopy*.

White Rose Research Online URL for this paper:
<https://eprints.whiterose.ac.uk/110415/>

Version: Accepted Version

Article:

Cascant, Mari Merce, Rubio, S, Gallelo, Gianni et al. (3 more authors) (2017) Prediction of alkaline earth elements in bone remains by near infrared spectroscopy. *Talanta*. pp. 428-434. ISSN 0039-9140

Reuse

This article is distributed under the terms of the Creative Commons Attribution-NonCommercial-NoDerivs (CC BY-NC-ND) licence. This licence only allows you to download this work and share it with others as long as you credit the authors, but you can't change the article in any way or use it commercially. More information and the full terms of the licence here: <https://creativecommons.org/licenses/>

Takedown

If you consider content in White Rose Research Online to be in breach of UK law, please notify us by emailing eprints@whiterose.ac.uk including the URL of the record and the reason for the withdrawal request.

1 **PREDICTION OF ALKALINE EARTH ELEMENTS IN BONE REMAINS BY NEAR INFRARED**
2 **SPECTROSCOPY**

3 Mari Merce Cascant, Sonia Rubio, Gianni Gallelo*, Agustín Pastor, Salvador Garrigues and
4 Miguel de la Guardia.

5 Department of Analytical Chemistry, University of Valencia,
6 50 Dr. Moliner Street, research building
7 46100 Burjassot, Valencia, Spain.

8 * Corresponding author
9

10 **Abstract**

11 An innovative methodological approach has been developed for the prediction of the
12 mineral element composition of bone remains. It is based on the use of Fourier Transform
13 Near Infrared (FT-NIR) diffuse reflectance measurements. The method permits a fast,
14 cheap and green analytical way, to understand post-mortem degradation of bones caused
15 by the environment conditions on different skeletal parts and to select the best preserved
16 bone samples. Samples, from the Late Roman Necropolis of Virgen de la Misericordia
17 street and En Gil street located in Valencia (Spain), were employed to test the proposed
18 approach being determined calcium, magnesium and strontium in bone remains and
19 sediments. Coefficients of determination obtained between predicted values and
20 reference ones for Ca, Mg and Sr were 90.4, 97.3 and 97.4, with residual predictive
21 deviation of 3.2, 5.3 and 2.3, respectively, and relative root mean square error of
22 prediction between 10 and 37%. Results obtained evidenced that NIR spectra combined
23 with statistical analysis can help to predict bone mineral profiles suitable to evaluate bone
24 diagenesis.

25 Keywords: NIR, multivariate statistics, alkaline earth elements, buried bones, diagenesis,
26 soil.

27

28

29 **1. Introduction**

30 Bone is composed of 50 to 70% mineral, 20 to 40% organic matrix, mainly collagen, 5 to
31 10% water, and less than 3% lipids. The mineral content of bone is mostly hydroxylapatite
32 $[\text{Ca}_{10}(\text{PO}_4)_6(\text{OH})_2]$, with small amounts of carbonate, magnesium, and acid phosphate, with
33 missing hydroxyl groups that are normally present [1]. Under physiologic conditions,
34 hydroxylapatite is the only stable mineral in bones and is composed of 38% of calcium and
35 18% of phosphorous, with trace of sodium (0,6%), magnesium and small amount of other
36 elements [2]. The number of ionic substitutions possible in biological apatite is smaller
37 than in geologic apatites due to the limited number of available elements in the body.
38 Among the substituting ions that are known and/or reported in bone and tooth mineral
39 are F^- , Cl^- , Na^+ , K^+ , Fe^{2+} , Zn^{2+} , Sr^{2+} , Mg^{2+} , citrate, and carbonate [3].

40 Minerals are ingested from food or involuntary absorbed from the environment. Chemical
41 composition of bones mineral is commonly employed to investigate pathologies, nutrition,
42 injuries and other bioarchaeological and forensic issues.

43 The mineral composition of bones can be post-mortem modified by post-depositional
44 processes, called as well diagenesis, and since many decades researchers have been
45 intensively studied these natural mechanisms. Some authors have evaluated post-mortem
46 soil contamination in bones [4-9]. Other authors have studied diagenesis and degradation
47 effects on bone matrix [10-13].

48 Calcium, oxygen and hydrogen are major constituents of mineral bones as hydroxylapatite
49 [14]. Strontium is a non-essential trace element that competes to replace calcium[15]and
50 has been linked to food consumption habits [16]. The soil composition and environmental
51 conditions play a crucial role in diagenesis, affecting the element concentration of the
52 buried bones.

53 The general aims of this study has been to develop a low cost, clean and fast strategy to
54 understand how post-mortem degradation in bones caused by the environment could
55 affect different skeletal parts and define an approach to select the best preserved bone
56 samples. Therefore, a method for the determination of mineral elements in bone remains
57 has been developed employing Fourier Transform Near Infrared (FT-NIR) spectroscopy by
58 using chemometric tools as principal component analysis (PCA) and Partial Least Square
59 (PLS). Inductively-Coupled Plasma Optical Emission Spectroscopy (ICP-OES) results have
60 been used as reference data to create prediction models.

61 ICP-OES has been commonly used as an accurate procedure to determine mineral
62 elements in soils and bones [17-21]. ICP-OES technique is very useful for multi-element
63 analysis. However it requires a previous sample digestion and dissolution, involving the
64 use of strong acids and providing non-degradable wastes. A green alternative to the
65 aforementioned technique could be infrared (IR) spectroscopy which provides fast
66 spectral acquisition, a cheap acquisition and maintenance cost and a sustainable method,
67 since it does not use reagents and can be employed directly on solid samples.
68 Combination of IR spectroscopy with chemometric data analysis could offer a significant

69 tool for the determination of major components of bones and sediments including
70 mineral elements.

71 Fourier Transform infrared (FT-IR) spectroscopy of bones has been used for various
72 applications as collagen determination, bone crystal size, some carbonates and crystalline
73 structure [22-25], and geochemical taphonomy [26] and as screening tool for diagenetic
74 alteration [27, 28]. On the other hand, only few studies have employed NIR for soils [29]
75 and bones analysis [30] in archaeological contexts.

76

77 In the present study, two hundred seventy one samples obtained from at least 78
78 individuals, have been analyzed. Samples belong to adult and young individuals and are
79 from the Late Roman Necropolis of Virgen de la Misericordia Street [19] and en Gil Street
80 [31], both located in the city of Valencia (Spain). The Late Roman burial rite consisted in
81 inhumation. At this sites, the tombs belong to the period from the I century A.D. until the
82 beginning of the V century A.D.

83 Bone samples were collected from femur, tibia, humerus, radius and parietal bones, which
84 were classified as cortical bones, and ribs as spongy bones. Furthermore, bone samples
85 from the outer bone layer and soil samples were analyzed. Outer bone layer samples were
86 obtained from the external bone surface directly in contact with the sediments. Principal
87 Component Analysis (PCA) was applied to identify bone samples with a well preserved
88 elemental composition. Therefore for the first time Partial Least Square (PLS) regression
89 models were built to predict the concentration of calcium, magnesium and strontium in
90 skeletal remains by NIR spectra of the mineralized and homogenized solid samples.

91

92 **2. Materials and methods**

93 **2.1. Sample collection**

94

95 Bone samples were collected from 78 different individuals, sampling around 5 cm of each
96 bone and the weight of the collected sample ranged between 15 and 20 grams depending
97 on the type of bone. Bones as femur, tibia, humerus, radius and parietals, mainly
98 composed by a cortical matrix were classified as “cortical”, and ribs mainly composed by a
99 spongy matrix were grouped as “spongy”. The first 2 mm of bone directly in contact
100 with the sediments was called external part of bones and was obtained employing a
101 bistoury to scrape. All bones were sampled avoiding the osteometric points, and the
102 sampling was carried out using a cutting toll and a micro spoon spatula.

103 To provide reproducible and comparable results compatible with the sensitivity of the
104 analytical methods employed and so appropriately relate NIR obtained data with the
105 reference method data all samples were previously mineralized in a muffle furnace,
106 (temperature programme employed: I. 30min at 150 °C; II. 1° /min up to 450 °C; III. 24h at
107 450 °C; IV. 30 °C), and pulverized and homogenized with an agate mortar

108

109 A total of 243 samples from Virgen de la Misericordia were analysed. Bone samples were
110 divided in three groups: i) internal part of bones, composed by the internal part of cortical
111 and spongy ones (95 samples), ii) external part of bones, composed by the first external
112 layer of cortical bones and spongy ones (94 samples) and, iii) sediments that were directly

113 in contact with the bones (54 samples). Additionally following the mentioned
114 classification, 28 samples from En Gil internal part of bones (8 samples), external part of
115 bones (10 samples) and sediments (10 samples) were also analyzed.

116

117 **2.2. Apparatus and methods**

118 For diffuse reflectance near infrared spectra acquisition, a Fourier transform near infrared
119 spectrometer, model Multipurpose Analyzer (MPA) from Bruker (Bremen, Germany),
120 equipped with an integrating sphere was employed. This instrument is equipped with a
121 NIR source, a quartz beamsplitter and PbS detector. For instrumental and measurement
122 control as well as for data acquisition, Opus 6.5 software from Bruker was used.

123

124 References values about the mineral composition of samples were determined by using an
125 Optima 5300 DV ICP-OES Perkin Elmer (Norwalk, CT, USA) equipped with an autosampler
126 AS 93-plus and a cross flow nebuliser. Samples were previously calcinated inside a muffle
127 furnace Biometra Lenton ECF 12145A (Lanera, España) and acid digested using a heating
128 plate Ika C-Mag HS7.

129

130 **2.3. Reference method**

131 The digestion method was developed modifying the process described by Gallelo et al.
132 2013 and 2014 [19] and consisted in addition to 0.5 g of mineralized sample of 1:1 HCl and
133 HNO₃ (using 37 % HCl and 69 % HNO₃ high purity stock) and digested in a water bath at
134 100° C. This concentrated solution (A), was diluted 1:250 obtaining solution (B), to

135 measure Mg and Sr. Solution (C) was obtained to analyze Ca by diluting 1:2000 solution
136 (A). Concentrations of HCl and HNO₃ have been maintained constant in all solutions. A
137 multi-element stock solution containing Ca, Mg and Sr at a concentration of 100 µg ml⁻¹
138 was employed for the preparation of the calibration standards in 50 ml volumetric flasks.
139 To avoid the obstruction of the nebulizer system samples were filtered employing filter
140 paper (Whatman™ N.1 of 70mm). Concentrations ranging between 0 and 20 µg ml⁻¹
141 were used for Ca, Mg and Sr. Standards were obtained from Sharlab S.L. (Barcelona,
142 Spain). The standard error of readings during the analysis ranged from 0 % to 2 % for the
143 major elements considered. Bone ash NIST 1400 and soil GBW07408 were used as
144 standard reference materials for evaluating the accuracy of the analytical method and Re
145 was used as internal standard. Mineral element content of studied samples, determined
146 by reference method, varied between 72 and 421 mg g⁻¹ for calcium, 998 and 10964 µg g⁻¹
147 for magnesium and, 102 and 2100 µg g⁻¹ for strontium.

148

149 **2.4. NIR procedure**

150 Pulverized mineralized samples were placed in clear glass vials of 11 mm internal diameter
151 and 25 mm height to directly obtain their NIR spectra by diffuse reflectance in Kubelka–
152 Munk units. Spectra were collected between 14000 and 4000 cm⁻¹ by averaging 50 scans
153 and using an optical resolution of 4 cm⁻¹. A background spectrum was acquired before
154 each series, from the closed integrating sphere using the same instrumental conditions
155 than those employed for samples measurement. Three measurements of each sample
156 were obtained by rotating the sample vial position between replicates in order to ensure a

157 good reliability. The average of the triplicate spectra of each sample was employed for
158 data exploration and to build the chemometric models.

159

160 **2.5. Chemometric data treatment**

161 Data treatment was carried out using in-house written functions employing Matlab
162 8.3.0.532 (R2014a) from Mathworks (Natick, MA, USA) being employed for Principal
163 Analysis Components (PCA) and Partial least squares (PLS) regression model, the PLS
164 Toolbox 7.5.2 from Eigenvector Research Inc. (Wenatchee, WA, USA).

165 PCA applied to IR spectra was used as data exploration; based on the distance between
166 samples the evaluation of their similarity. PLS models were applied to spectral data to
167 develop prediction models for Ca, Mg and Sr. These calibration models were developed
168 based on the statistically inspired modification of the PLS method (SIMPLS) algorithm
169 [32]. To select the most appropriate sample calibration set, Kennard–Stone (KS)
170 algorithm [33] was used, thus selecting a representative subset to ensure training
171 samples spread evenly throughout the sample space. For building the best PLS models,
172 different spectral regions and spectra pre-treatments were tested as multiplicative
173 scatter correction (MSC), standard normal variation (SNV), a Savitzky-Golay first (FD) and
174 second derivative (SD), and mean center (MC) also combination of them. The
175 performance of PLS-NIR models was evaluated according to the root mean square error
176 of cross validation and prediction (RMSECV and RMSEP) values, the coefficient of
177 determination for prediction (R^2_{pred}), relative root mean square error of prediction
178 (RRMSEP) and residual predictive deviation (RPD), calculated this last parameter as the

179 ratio between standard deviation (SD) of the prediction set and the RMSEP values [34].
180 Generally, RPD value greater than 3.0 is considered adequate for analytical purposes with
181 excellent prediction accuracy, between 2.5 and 3.0 implies that the model has a good
182 precision and between 2.0 and 2.5 indicates that the model has an approximate
183 precision. A value for the RPD between 1.5 and 2.0 reveals a possibility to distinguish
184 between high and low values and a RPD 1.5 indicates that the calibration is not usable
185 [35]. The optimum number of latent variables (LV's) was determined by cross-validation
186 using leave one out sample in order to obtain the minimum value of RMSECV.

187

188 **3. Results and discussion**

189 ***3.1. FT-NIR spectra***

190 Figure 1 shows, in Kubelka Munk units, the averaged NIR spectra of a) internal part, b)
191 external part of bones and c) sediment samples, considered in this study without any data
192 pre-treatment, in the region between 9000 and 4000 cm^{-1} . These sample spectra present
193 differences in the intensity and position of certain bands, but all show absorption bands
194 around 7200 and 5220 cm^{-1} related to combination vibrations of H–O–H bend and O–H
195 stretch of water. The main difference which presents internal bones is the weak vibration
196 which appear near 4655 cm^{-1} (without a clear assignment) and the absorption near 6977
197 cm^{-1} assigned to the first overtone of the stretching vibrations of OH group in
198 hydroxyapatite [36], that is higher than in external part of bones. In the case of the
199 sediment samples, the aforementioned band is absent. Additionally, at 5278 cm^{-1} , internal
200 part of bone and external part of bone in minor intensity, present an absorption band

201 related to apatite [30]. On the other hand, in sediment samples it is present a band at
202 7070 cm^{-1} related to the first overtone of the O–H stretch vibration in metal–O–H [37].
203 Moreover, vibrations bands near of 4530 cm^{-1} are due to clay minerals, like smectite and
204 illite, and the band at 4265 cm^{-1} is associated with the contribution of calcite [37], which
205 decreases in intensity in external bone. In the case of internal part of bone samples, the
206 band located at 4265 cm^{-1} not appears and the band at 4530 cm^{-1} is less intense than in
207 external part of bones. So that, in external part of bones appear typical bands of sediment
208 samples related with metal-OH (7070 cm^{-1}), calcite (4265 cm^{-1}) and clay minerals (4530
209 cm^{-1}), and lower bands of hydroxyapatite (6977 cm^{-1}) and apatite (5278 cm^{-1}).
210 Degradation of hydroxyapatite in external part of bones is a great indicator of diagenetic
211 process. Sediments around bones are crucial role to conservation of them, and sediments
212 analysis should be carried out in order to assess their contribution to the modification of
213 the bone chemical composition.

214

215

216 **3.2. Data Exploration by PCA**

217 Before building the calibration models, PCA was used for exploratory data analysis to
218 study the spectral differences between considered samples. Figure 2 presents the scores
219 plot for first and the second principal components obtained from PCA for Misericordia and
220 En Gil Necropolis, after a) FD and MC and b) MSC, FD and MC pre-treatment, being
221 selected the region from 9014 to 4000 cm^{-1} . In Figure 2a, the two first principal
222 components after spectra pretreatment by using FD and MC represent 86.07% of the

223 explained variance, being 76.93 and 9.14% for PC1 and PC2, respectively. In the scores
224 plot, there is not a clear-cut grouping of samples, but it can be appreciated that sediment
225 samples spectra are clearly different from those of internal part of bone samples and that,
226 external part of bone samples are located between sediment and internal part of bone
227 ones in the direction of PC1. In Figure 2b, it can be seen that the scores plot for first and
228 the second principal components after MSC, FD and MC pretreatment, represent 85.72%
229 of the explained variance (PC1 corresponds to 80.49% and PC2 corresponds to 5.23% of
230 the variance). It can be seen that internal part of bone samples are located towards the
231 right of the PC1 and sediment samples are dispersed in the left. External part of bone
232 samples are situated between these two groups in the direction of PC1. Moreover, PCA
233 indicates that samples derived from En Gil are similar to Misericordia samples, and
234 because of that samples from Misericordia can be used as calibration set to predict
235 alkaline earth elements in En Gil samples.

236 The aforementioned PCAs were built using differentiated internal and external parts of
237 bones in both, spongy and cortical remains. Figure 2c presents the scores plot after FD and
238 MC and Figure 2d after MSC, FD and MC pretreatment. No differences were detected
239 between internal parts of cortical and spongy bones. However if we look at the external
240 part of bones, spongy group is located near to sediment samples, and external part of
241 cortical bones are located close to internal part of bones because spongy tissues are more
242 susceptible to diagenesis than cortical [38] due to the fragility and porosity of their
243 structure. Wavenumbers responsible for the distinction of the samples in PCA can be

244 identified in the corresponding loading plots (Figure 2e and 2f) with a clear identification
245 of bands around 7000 cm^{-1} and between 5500 and 4000 cm^{-1} .

246

247 So, it can be concluded that PCA analysis using NIR spectra data provides a fast and green
248 tool to identify changes caused by the environment in bone samples. These results
249 indicate that external part of bones suffer an increased degradation produced by
250 diagenetic factors than internal part of bones, especially in the case of spongy bones
251 external part due to their high porosity. Consequently, conclusions about identification of
252 biogenetic signals using major element ratios could change depending of the bone class
253 evaluated. To avoid mistakes, the use of PCA analysis, as exploratory method, permits a
254 prior selection of samples, not affected by diagenetic processes, to be used in different
255 bioarchaeological and forensic studies involved in bone analyses. Additionally, PCA is a
256 good indicator to test if the calibration set contains the validation samples in order to be
257 used in PLS models without errors due to extrapolation of data.

258

259 **3.3. PLS-NIR models**

260 To build PLS models, Misericordia samples were divided into a calibration and a validation
261 subset with 183 and 60 objects, respectively, using K-S algorithm for the training set
262 selection, composed by 62 external part of bones, 70 internal part of bones and 51
263 sediment samples.

264 The main characteristics of calibration and validation sets selected for the three elements
265 determination by PLS-NIR are indicated in Table 1. Several regions and different pre-

266 processing strategies were assayed to build the best models and to evaluate their
267 prediction capability. For all elements, regions selected were those between 9014 and
268 4000 cm^{-1} . To build PLS-NIR models using the selected spectral range, 3, 4 and 4 LVs were
269 employed for Ca, Mg and Sr, respectively, in order to minimize the RMSECV, explaining
270 89.1 %, 90.8 % and 88.5 % of the total variance of the X data block and 92.4%, 95.0% and
271 90.4% of the Y data block, respectively. For Ca and Mg, FD with a window of 11 points and
272 a second order polynomial, and MC treatment were adopted as signal pre-processing. For
273 strontium, MSC, FD and MC were chosen. Additionally, concentration data were mean
274 centered as well in all cases. Outliers can be identified by Q residual versus the Hotelling
275 T^2 values, being removed 2 samples from the calibration set of Ca, Mg and Sr and 2
276 samples from the validation set of Ca and Sr and only one sample of Mg, prior to do the
277 calculations and validation of the final PLS models for those elements. Figure 3a shows the
278 regression between PLS-NIR predicted values for Ca, Mg and Sr and those obtained by the
279 reference ICP-OES method. It can be seen that calibration and validation sample points
280 were closely distributed near the optimum regression line between predicted and
281 measured values for the three elements, obtaining high coefficients of determination for
282 calibration (R^2_{cal}), cross validation (R^2_{CV}) and prediction (R^2_{pred}) in all elements. The
283 prediction capability of PLS-NIR models were good for all elements, obtaining RRMSEP
284 values of 10%, 15% and 19% for calcium, magnesium and strontium, respectively. The
285 most important calibration and validation parameters of the developed PLS-NIR models
286 are summarized in Table 2.

287

288 It can be seen that samples of internal part of bones contain higher calcium ($368 \pm 24 \text{ mg}$
289 g^{-1}) and strontium ($1306 \pm 235 \text{ } \mu\text{g g}^{-1}$) levels and lower magnesium content ($1393 \pm 175 \text{ } \mu\text{g}$
290 g^{-1}) than external parts (with $261 \pm 47 \text{ mg g}^{-1}$ of Ca, $844 \pm 203 \text{ } \mu\text{g g}^{-1}$ of Sr and 5599 ± 1684
291 $\text{ } \mu\text{g g}^{-1}$ of Mg) and sediment samples (with $133 \pm 17 \text{ mg g}^{-1}$ of Ca, $239 \pm 60 \text{ } \mu\text{g g}^{-1}$ of Sr and
292 $8165 \pm 858 \text{ } \mu\text{g g}^{-1}$ of Mg). As aforementioned, in physiologic conditions, hydroxylapatite is
293 composed of 38 % Ca, with traces of Mg and small amounts of other elements like Sr,
294 indicating that internal part of bones are intact looking at Ca values that are around
295 the 38%. Mg enrichment in external part of bones indicates that this element is probably
296 incorporated into the bones from sediments during diagenesis process.

297 External part of bones, especially in the case of spongy bone remains are more sensitive to
298 diagenetic processes caused by the environment indicating that degradation not affects in
299 the same extent different skeletal parts. Due to the fact that spongy bones have higher
300 porosity and thinner cortex than cortical bones, the first type is less resistant to diagenetic
301 factors suffering chemical changes.

302

303 Results obtained by PLS-NIR models indicated that NIR spectroscopy has a good potential
304 to predict alkaline earth elements content in bone remains. As mentioned this method has
305 many advantages over the conventional employed analytical techniques because it is
306 quick, inexpensive, non-destructive for pulverized samples and does not require the use of
307 chemical reagents nor solvents.

308

309 **3.4. PLS-NIR prediction capability**

310 To evaluate the PLS-NIR prediction capability of models built to predict Ca, Mg and Sr
311 concentrations in bones and sediments, an independent validation set, not employed
312 during the calibration step, was used. For this propose external part, internal part of
313 bones and sediment samples of En Gil Necropolis were used as external set. The mean,
314 concentration range and standard deviation for the concentration of analysed elements
315 employed for prediction set are summarized in Table 1. Predicted values of the analytes
316 versus those obtained by the reference methods are shown in Figure 3b and the most
317 important calibration and prediction parameters of the developed NIR-PLS models are
318 summarized in Table 2. Acceptable RRMSEP values were obtained for calcium and
319 magnesium with 15% and 11%, respectively, and for strontium a value of 37% was
320 obtained, with correlation coefficients of 90.4, 97.4 and 97.4, and RPD values of 3.2, 5.33
321 and 2.3, respectively. These results demonstrate a good predictive capability of the PLS-
322 NIR models developed to evaluate alkaline earth elements in bones and sediment
323 samples.

324

325 Furthermore it must be indicated the PLS models were made from bone samples of
326 different origin, and date of those of the training set, confirming the feasibility of our
327 innovative methodological proposal for the evaluation of alkaline earth elements in
328 archaeological remains.

329

330 The obtained results indicate a good predictive capability for Mg in samples that not
331 belong to the same population while Ca were predicted with relative errors of 15% and Sr

332 37%, respectively, being thus limited as a screening tool. Especially for Sr the high relative
333 error of 37% is probably due to the lower levels of this element found in some samples
334 not compatible with the sensitivity of NIR.

335

336

337 **4. Conclusions**

338 Fourier Transform Near Infrared (FT-NIR) provides a fast, cheap and green analytical
339 method for the prediction of the content of calcium, magnesium and strontium in buried
340 bone and sediment samples, and it could be very useful to understand post-mortem
341 changes of bones caused by the environment which can affects different skeletal parts
342 and for selecting bone samples with well preserved biogenetic signals. PCA has shown that
343 the alkaline earth element profile of bone and soil samples, as expected, is clearly
344 different. Furthermore the external surface of spongy bones is more similar to the soils
345 than to the surface of cortical bones. This confirm that the outer bone layer of spongy
346 bones is more altered than the cortical surface and the presence of Ca, Mg and Sr is
347 similar to that of soil samples of the studied sites. Therefore it can be concluded that
348 environmental factors have a main impact on spongy tissues, which are more susceptible
349 to diagenetic processes, than on the cortical bones. It is indicated in the NIR spectra by the
350 loss of apatite band (the main bone compound) and the presence of clay bands especially
351 on spongy bone surface.

352 A milestone in the study of bone remains is settled in this work by the development of
353 PLS-NIR models, indicating that FT-NIR spectroscopy can be employed to predict Ca, Mg

354 and Sr contents in bones remains and soils samples. Ca and Sr contents were found to be
355 higher in the internal part of bone samples, opposite to Mg contents that were higher in
356 the external bone surface and soils, and lower in internal part of bones. Our developed
357 methodological approach combines NIR spectroscopy and statistical analysis and this
358 allowed us to predict bone alkaline earth mineral composition opening a new perspective
359 for the identification of better preserved samples in bioarchaeological studies and forensic
360 science investigations.

361 Regarding the limitations of the study it must be noticed that it was based only on the
362 mineral part of skeletal remains which were treated thermally and pulverized before
363 measurements thus losing information from the organic part of bones and soils.
364 Additionally, the lack of sensitivity of NIR spectroscopy seriously affected the capability of
365 these measurements to be employed for trace element determination and just important
366 elements present as major components of bones, like Ca, Mg and Sr could be determined.

367

368 **Acknowledgements**

369 Authors acknowledge the financial support of Generalitat Valenciana (Project **PROMETEO**
370 **II/2014/077**) and **Ministerio de Economía y Competitividad-Feder** (Projects **CTQ 2014-**
371 **52841-P** and **CTQ 2012-38635**). M.C acknowledges the FPI grant (**BES-2012-055404**)
372 provided by the **Ministerio de Economía y Competitividad** of the Spanish government.

373 The authors would like to thanks all the students of Chemistry and Archaeology which
374 have contributed to the realization of this study.

375

377 **References**

- 378 [1] B. Clarke, Normal bone anatomy and physiology, *Clin. J. Am. Soc. Nephrol.* 3 (2008) Suppl 3,
379 S131–139.
- 380 [2] J. Burton, Bone chemistry and trace element analysis. in M.A. Katzenberg, S.R. Saunders
381 (Eds.) *Biological anthropology of the human skeleton*. 2nd ed. John Wiley & Sons, Inc.,
382 Hoboken, NJ (2008) 443–460.
- 383 [3] B. Wopenka and J. D. Pasteris, A mineralogical perspective on the apatite in bone, *Mater. Sci.*
384 *Eng. C*, 25 (2005) 131–143.
- 385 [4] R. E. M. Hedges and A. R. Millard, Bones and Groundwater: Towards the Modelling of
386 Diagenetic Processes, *J. Archaeol. Sci.*, 22 (1995) 155–164.
- 387 [5] R. E. M. Hedges, Bone diagenesis: an overview of processes, *Archaeometry*, 44 (2002) 319–
388 328.
- 389 [6] W. Querido, A. L. Rossi, and M. Farina, The effects of strontium on bone mineral: A review on
390 current knowledge and microanalytical approaches, *Micron*, 80 (2016), 122–134.
- 391 [7] J. B. Lambert, L. Xue, and J. E. Buikstra, Inorganic analysis of excavated human bone after
392 surface removal, *J. Archaeol. Sci.*, 18 (1991) 363–383.
- 393 [8] F. Donald Pate and J. T. Hutton, The Use of Soil Chemistry Data to Address Post-mortem
394 Diagenesis in Bone Mineral, *J. Archaeol. Sci.*, 15 (1988) 729–39.
- 395 [9] J. Zapata, C. Pérez-Sirvent, M. Martínez-Sánchez, and P. Tovar, Diagenesis, not biogenesis:
396 Two late Roman skeletal examples, *Sci. Total Environ.*, 369 (2006) 357–368.
- 397 [10] I. Reiche, L. Favre-Quattropiani, Calligaro, T. J. S., H. Bocherens, L. Charlet, M. Menu, Trace
398 element composition of Archaeological Bones and postmortem alteration in the burial
399 environment. *Nuclear Instruments and Methods. Physics Research B* 150 (1999) 656-662.
- 400 [11] I. Reiche, L. Favre-Quattropiani, C. Vignaud, H. Bocherens, L. Charlet, M. Menu, A multi-
401 analytical study of bone diagenesis: the Neolithic site of Bercy (Paris, France). *Meas. Sci.*
402 *Technol.* 14 (2003)1608-1619.
- 403 [12] T.H. Schmidt-Schultz, M. Schultz, Intact protein molecules in archaeological bones – Bone
404 matrix as a treasure chest of ancient diseases and living conditions. *American Journal of*
405 *Physical Anthropology. Annual Meeting Issue* 1999, Wiley-Liss, p. 230.
- 406 [13] T. A. Surovell and M. C. Stiner, Standardizing Infra-red Measures of Bone Mineral
407 Crystallinity: an Experimental Approach, *J. Archaeol. Sci.*, 28(2001) 633–642.
- 408 [14] F. Ignac, G. Gopinath, and V. der W. Hans, *Radionuclide and Hybrid Bone Imaging*. Springer
409 Heidelberg New York Dordrecht London, 2012.

- 410 [15] M. L. Carvalho and A. F. Marques, Diagenesis evaluation in Middle Ages human bones using
411 EDXRF, X-Ray Spectrom., 37 (2008) 32–36.
- 412 [16] D. Guimarães, A. A. Dias, M. Carvalho, M. L. Carvalho, J. P. Santos, F. R. Henriques, F. Curate,
413 and S. Pessanha, Quantitative determinations and imaging in different structures of buried
414 human bones from the XVIII-XIXth centuries by energy dispersive X-ray fluorescence –
415 Postmortem evaluation, Talanta, 155 (2016) 107–115.
- 416 [17] G. Gallelo, J. Kuligowski, A. Pastor, A. Diez, and J. Bernabeu, Biological mineral content in
417 Iberian skeletal remains for control of diagenetic factors employing multivariate statistics, J.
418 Archaeol. Sci., 40(2013) 2477–2484.
- 419 [18] A.-F. Maurer, M. Gerard, A. Person, I. Barrientos, C. R. del, V. Darras, C. Durlet, V. Zeitoun, M.
420 Renard, and B. Faugère, Intra-skeletal variability in trace elemental content of Precolumbian
421 Chupicuaro human bones: The record of post-mortem alteration and a tool for palaeodietary
422 reconstruction, J. Archaeol. Sci., 38 (2011) 1784–1797.
- 423 [19] G. Gallelo, J. Kuligowski, A. Pastor, A. Diez, and J. Bernabeu, Chemical element levels as a
424 methodological tool in forensic science, J Forensic Res, 6 (2014) 1000264.
- 425 [20] A.-F. Maurer, A. Person, T. Tütken, S. Amblard-Pison, and L. Ségalen, Bone diagenesis in arid
426 environments: An intra-skeletal approach, Palaeogeogr. Palaeoclimatol. Palaeoecol., 416
427 (2014) 17–29.
- 428 [21] S. Dal, L. Maritan, D. Usai, I. Angelini, and G. Artioli, Bone diagenesis at the micro-scale: Bone
429 alteration patterns during multiple burial phases at Al Khiday (Khartoum, Sudan) between
430 the Early Holocene and the II century AD, Palaeogeogr. Palaeoclimatol. Palaeoecol.,
431 416(2014) 30–42.
- 432 [22] S. W. Keenan, A. S. Engel, A. Roy, and G. Lisa Bovenkamp-Langlois, Evaluating the
433 consequences of diagenesis and fossilization on bioapatite lattice structure and composition,
434 Chem. Geol., 413 (2015) 18–27.
- 435 [23] C. N. Trueman, K. Privat, and J. Field, Why do crystallinity values fail to predict the extent of
436 diagenetic alteration of bone mineral?, Palaeogeogr. Palaeoclimatol. Palaeoecol., 266
437 (2008)160–167.
- 438 [24] T. J. U. Thompson, M. Islam, K. Piduru, and A. Marcel, An investigation into the internal and
439 external variables acting on crystallinity index using Fourier Transform Infrared Spectroscopy
440 on unaltered and burned bone, Palaeogeogr. Palaeoclimatol. Palaeoecol., 299(2011) 168–
441 174.
- 442 [25] T. J. U. Thompson, M. Islam, and M. Bonniere, A new statistical approach for determining the
443 crystallinity of heat-altered bone mineral from FTIR spectra, J. Archaeol. Sci., 40 (2013) 416–
444 422.
- 445 [26] G. Iliopoulos, N. Galanidou, S. A. Pergantis, V. Vamvakaki, and N. Chaniotakis, Identifying the
446 geochemical taphonomy of the osteological material from Katsambas rockshelter, J.
447 Archaeol. Sci., 37 (2010) 116–123.

- 448 [27] L. E. Wright and H. P. Schwarcz, Infrared and Isotopic Evidence for Diagenesis of Bone Apatite
449 at Dos Pilas, Guatemala: Palaeodietary Implications, *J. Archaeol. Sci.*, 23 (1996) 933–944.
- 450 [28] D. Alfano, A. R. Albunia, O. Motta, and A. Proto, Detection of diagenetic alterations by
451 Spectroscopic Analysis on Archaeological Bones from the Necropolis of Poseidonia
452 (Paestum): A case study, *J. Cult. Herit.*, 10 (2009) 509–513.
- 453 [29] J. Linderholm and P. Geladi, Classification of archaeological soil and sediment samples using
454 near infrared techniques, *NIR News*, 23 (2012) 6.
- 455 [30] D. Thomas, C. McGoverin, A. Chinsamy, and M. Manley, Near infrared analysis of fossil bone
456 from the Western Cape of South Africa, *J. Infrared Spectrosc.*, 19(2011) 151.
- 457 [31] G. Gallelo, S. Silvia, J. Kuligowski, B. Fulvio, M. Francesco, and P. Agustín, Variación química
458 intraesquelética relacionada con la diagénesis en los restos óseos de c/ en Gil (Valencia),
459 *SAGVNTVM*, 47 (2015) 175–186.
- 460 [32] S. de Jong, SIMPLS: An alternative approach to partial least squares regression, *Chemom.*
461 *Intell. Lab. Syst.*, 3 (1993) 251–263.
- 462 [33] R. W. Kennard and L. A. Stone, Computer Aided Design of Experiments, *Technometrics*, 11
463 (1969) 137–148.
- 464 [34] P.C. Williams, D. Sobering, How do we do it: A brief summary of the methods we use in
465 developing near infrared calibrations, A.M.C. Daves, P.C. Williams (Eds.), *Near infrared*
466 *spectroscopy: The future waves*, NIR Publications, Chichester, UK (1995) 185–188.
- 467 [35] W. Saeys, A. M. Mouazen, and H. Ramon, Potential for Onsite and Online Analysis of Pig
468 Manure using Visible and Near Infrared Reflectance Spectroscopy, *Biosyst. Eng.*, 91(2005)
469 393–402.
- 470 [36] Y. Ning, J. Li, W. Cai, and X. Shao, Simultaneous determination of heavy metal ions in water
471 using near-infrared spectroscopy with preconcentration by nano-hydroxyapatite,
472 *Spectrochim. Acta. A. Mol. Biomol. Spectrosc.*, 96 (2012) 289–294.
- 473 [37] V. Aranda, A. Domínguez-Vidal, F. Comino, J. Calero, and M. J. Ayora-Cañada, Agro-
474 environmental characterization of semi-arid Mediterranean soils using NIR reflection and
475 mid-IR-attenuated total reflection spectroscopies, *Vib. Spectrosc.*, 74 (2014) 88–97.
- 476 [38] J.B. Lambert, S.M. Vlasak, A.C. Thometz, J.E. Buikstra, A comparative study of the chemical
477 analysis of ribs and femurs in Woodland population, *American Journal of Physical*
478 *Anthropology* 59 (1982) 289-294.
- 479

Graphical Abstract

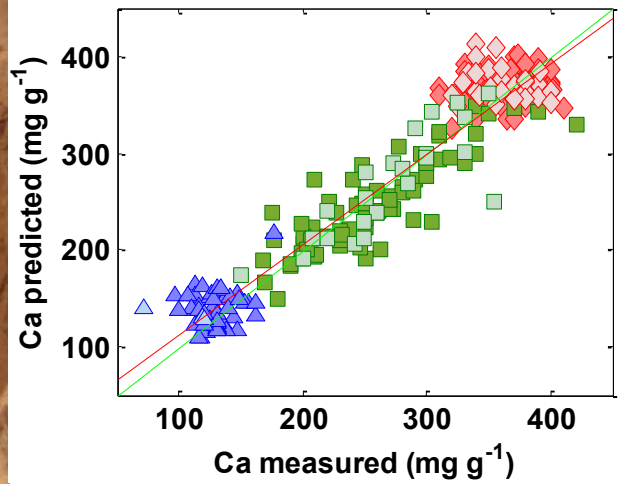
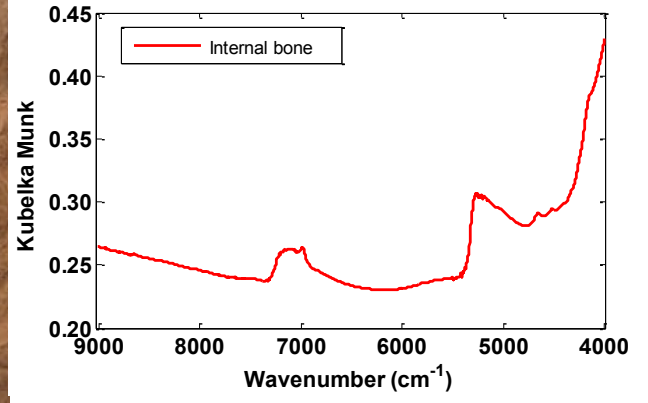


Table 1. Concentration ranges of determined mineral elements in calibration, validation and prediction data sets

Analyte	Set	Samples	Range	Mean value	SD
Calcium (mg g ⁻¹)	Calibration	181	96 - 421	260	100
Magnesium (µg g ⁻¹)		181	1050 - 10500	4967	3091
Strontium (µg g ⁻¹)		181	153 - 2100	823	486
Calcium (mg g ⁻¹)	Validation	58	72 - 400	312	76
Magnesium (µg g ⁻¹)		59	1070 - 8500	3226	2545
Strontium (µg g ⁻¹)		58	124 - 2010	1058	405
Calcium (mg g ⁻¹)	Prediction	26	112 - 421	233	114
Magnesium (µg g ⁻¹)		26	998 - 10964	6723	3864
Strontium (µg g ⁻¹)		26	102 - 1350	518	442

SD: Standard deviation

Table 2. Description of the best PLS-NIR models employed for the determination of Ca, Mg and Sr and their main figures of merit.

Element	Pre-process	LV	Misericordia samples								en Gil samples						
			RMSEC	R ² Cal	RMSECV	R ² CV	RMSEP	R ² Pred	RRMSEP (%)	RPD	RMSEP	R ² Pred	Slope	Intercept	Bias	RRMSEP (%)	RPD
Calcium (mg g ⁻¹)	FD, MC	3	27.5	92.4	29.0	91.6	31.7	83.4	10.2	2.4	35.6	90.4	0.8299	41.4	1.7	15.3	3.2
Magnesium (μg g ⁻¹)	FD, MC	4	686.3	95.0	750.2	94.1	496.6	96.3	15.4	5.1	723.7	97.3	0.9504	246.2	-81.3	10.8	5.3
Strontium (μg g ⁻¹)	MSC, FD, MC	4	150.1	90.4	169.8	87.7	198.9	76.2	18.8	2.0	198.9	97.4	0.9041	78.9	155.0	37.3	2.3

LV: number of latent variables

RMSEC: Root mean square error of calibration; RMSECV: Root mean square error of cross validation; RMSEP: Root mean square error of prediction; RRMSEP: Relative root mean square error of prediction; R² Cal: coefficient of determination of calibration; R² CV: coefficient of determination of cross validation; R² Pred: coefficient of determination of prediction.

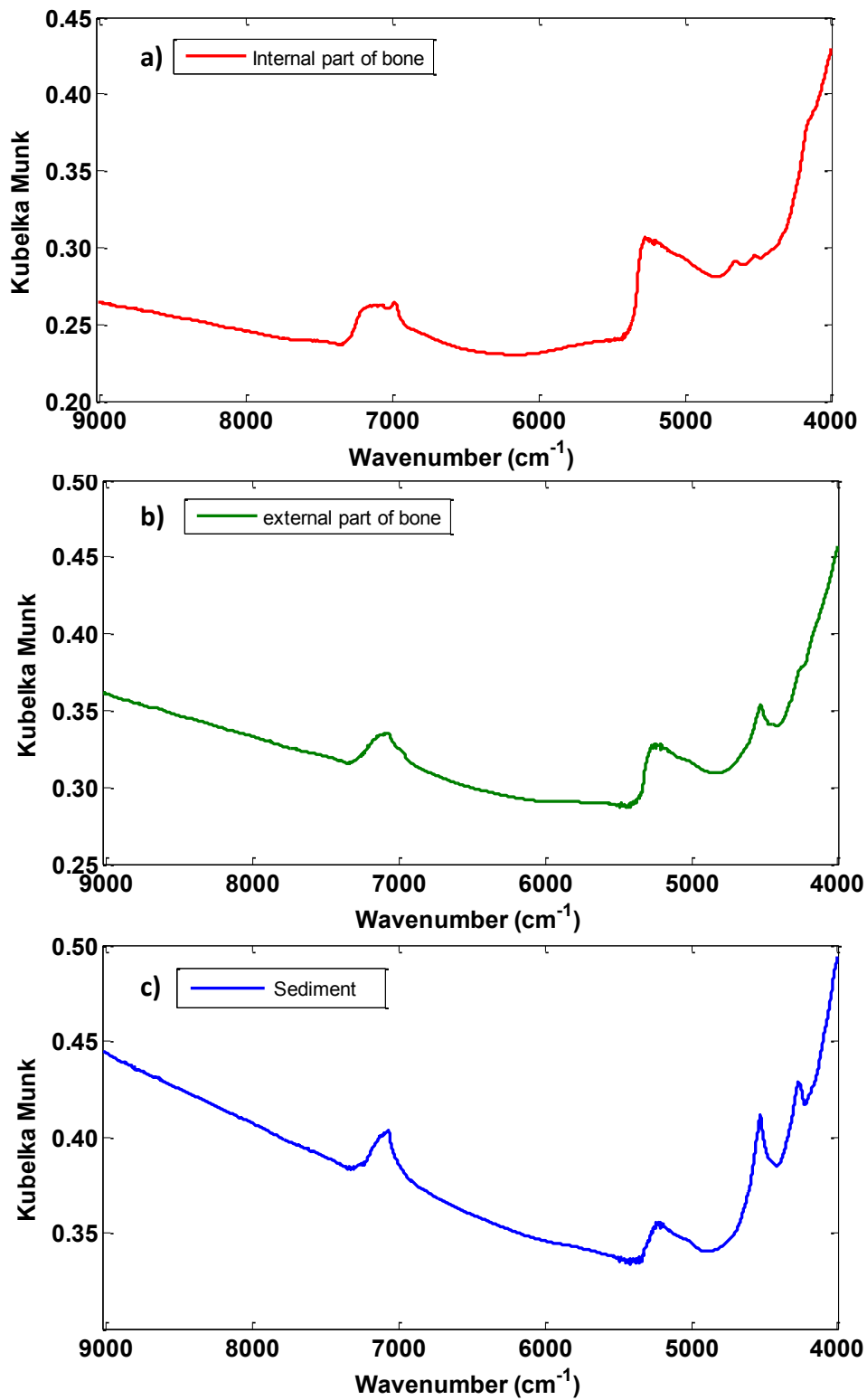


Figure 1. Averaged NIR spectra of mineralized bone and sediment samples comparing a) internal part, b) external part, and c) sediment samples. Note: Spectra were in Kubelka Munk units in the region between 9000 and 4000 cm⁻¹.

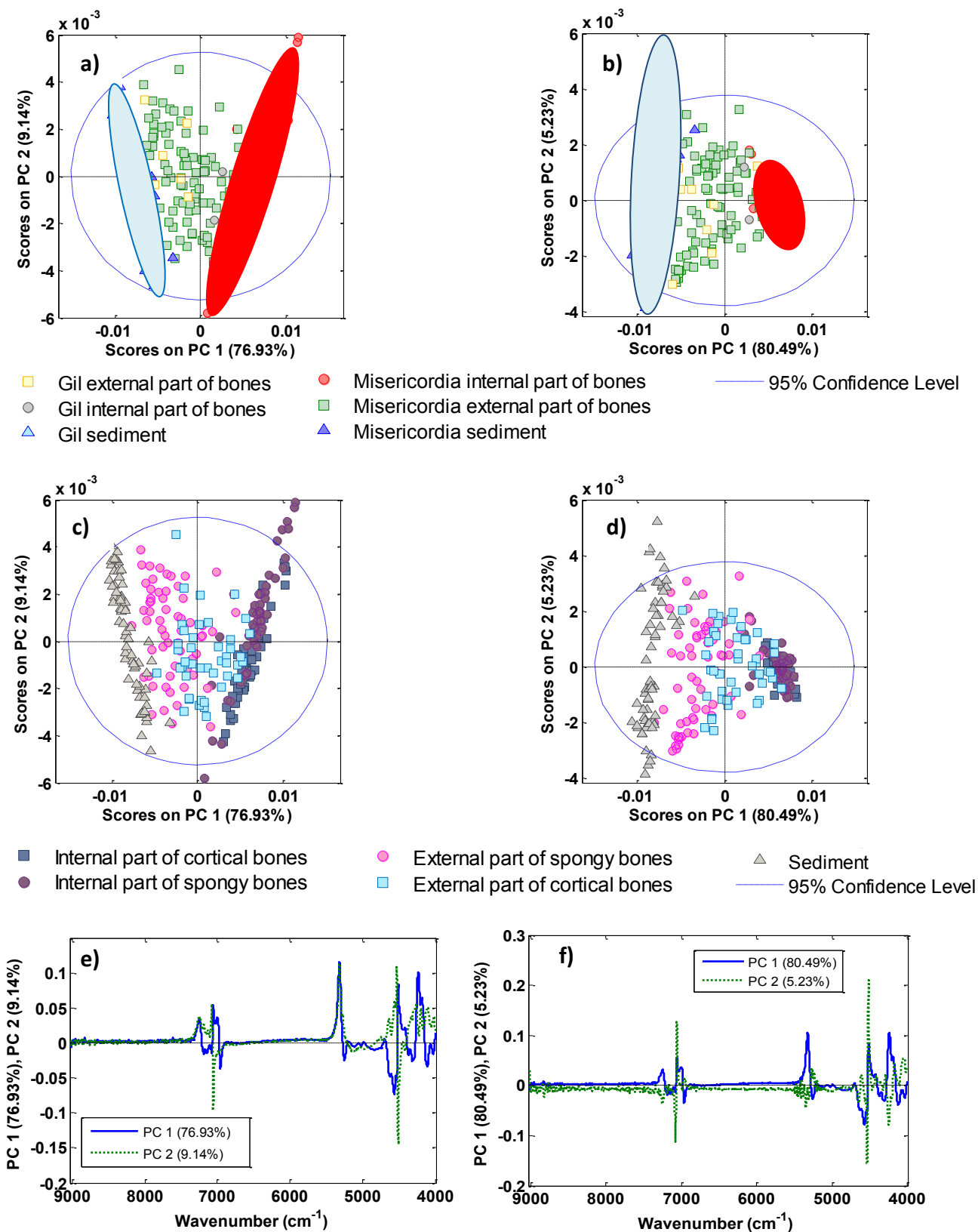


Figure 2. PLS scores and loadings graphs obtained after different spectra treatments. Score plots according Misericordia and En Gil Necropolis sample classification after: **a)** FD and MC, and **b)** MSC, FD and MC pretreatment. Score plots on considering the bone parts after: **c)** FD and MC, and **d)** MSC, FD and MC pretreatment. Loadings of PC1 and PC2 after: **e)** FD and MC, **f)** MSC, FD and MC pretreatment.

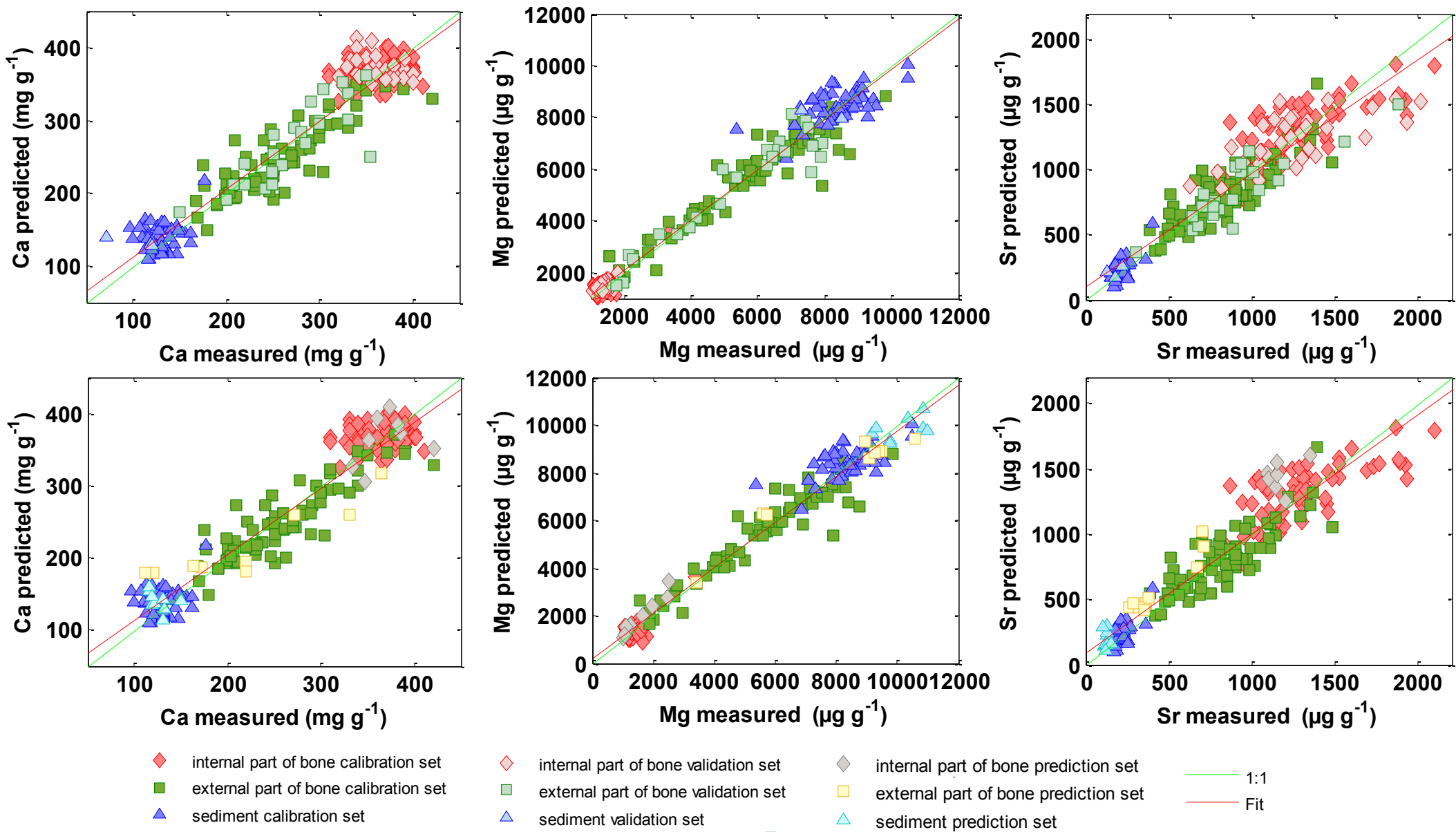


Figure 3. Regression between predicted and reference values obtained for the PLS-NIR determination of calcium, magnesium and strontium in bone remains and sediments